Atmos. Chem. Phys. Discuss., 12, 26477–26502, 2012
www.atmos-chem-phys-discuss.net/12/26477/2012/
doi:10.5194/acpd-12-26477-2012

Atmospheric Chemistry and Physics Discussions

Tropospheric impact of methane emissions from clathrates in the Arctic Region

S. Bhattacharyya[1], P. Cameron-Smith[1], D. Bergmann[1], M. Reagan[2], S. Elliott[3], and G. Moridis[2]

[1]Lawrence Livermore National Laboratory, Livermore, CA, USA
[2]Lawrence Berkeley National Laboratory, Berkeley, CA, USA
[3]Los Alamos National Laboratory, Los Alamos, NM, USA

Received: 4 September 2012 – Accepted: 23 September 2012 – Published: 5 October 2012

Correspondence to: S. Bhattacharyya (bhattacharyy1@llnl.gov)

Published by Copernicus Publications on behalf of the European Geosciences Union.

Abstract

A highly potent greenhouse gas, methane, is locked in the solid phase as ice-like deposits containing a mixture of water and gas (mostly methane) called clathrates in both ocean sediments and underneath permafrost regions. Clathrates are stable under high pressures and low temperatures. In a warming climate, increases in ocean temperatures could lead to dissociation of the clathrates and release methane into the ocean and subsequently the atmosphere. This is of particular importance in the shallow parts of the Arctic Ocean, since clathrates are expected to start outgassing abruptly at depths of around 300 m. In this paper, we present a comparison of simulations from the Community Earth System Model (CESM1) for present-day conditions with and without additional methane emissions from a plausible clathrate release scenario based on a state-of-the-art ocean sediment model. The CESM model includes a fully interactive physical ocean and we added a fast atmospheric chemistry mechanism that represents methane as a fully interactive tracer (with emissions rather than concentration boundary conditions) along with the main chemical reactions for methane, ozone, and nitrous oxide. The results show that such Arctic clathrate emissions increase methane concentrations non-uniformly, and that increases in surface ozone concentrations are greatest in polluted regions. We also find that the interannual variability in surface methane and ozone increases.

1 Introduction

Methane is widely understood (1) as the second most consequential greenhouse gas (after CO_2), (2) to be well mixed because of its long lifetime, and (3) to have sources in the Arctic that may be released in a warming climate. Methane clathrates (also known as hydrates) are solid crystalline compounds in which methane gas molecules (and perhaps other small molecules) are lodged within the lattices of water clathrate crystals. Sub-seabed methane is primarily produced by microbial and thermogenic

ACPD
12, 26477–26502, 2012

processes. Sea floor perturbations of temperature and pressure can then lead to release of methane clathrates (Elliott et al., 2010, 2011a; Reagan and Moridis, 2007, 2008, 2009; Reagan et al., 2011a; Archer, 2007; Archer et al., 2009; Kennett et al., 2000). A vast quantity of methane clathrate is estimated to be trapped in the marine sediments on continental margins and in permafrost regions. Precise estimates vary between $(0.5–3) \times 10^6$ Tg(CH_4) (Milkov, 2004; Archer et al., 2009) at the lower end, to an upper estimate of about 74.4×10^6 Tg(CH_4) (Klauda and Sandler, 2005; Gornitz and Fung, 1994), plus 2×10^6 Tg(CH_4) in methane bubbles (Buffett and Archer, 2004). The Arctic region alone is estimated to have a clathrate reservoir of about 0.53×10^6 Tg(CH_4) (Maslin et al., 2010), with a similar amount in the Antarctic (Wadham et al., 2012). There are also other potentially large sources of methane in the Arctic that could impart methane to the atmosphere in a warming scenario, particularly permafrost, the East Siberian Arctic Shelf, northern lakes, rivers, and wetlands (Stolaroff et al., 2012; Archer, 2007). Any release of that methane is then expected to produce radiative forcing that is enhanced by an increase in methane lifetime, ozone, stratospheric water vapor, and carbon dioxide (Isaksen et al., 2011, and references therein).

The potential impact of methane clathrates is shown in several paleoclimate studies (Lunt et al., 2010, 2011; Lamarque et al., 2006, 2007; Archer, 2007; Archer et al., 2009) which postulate the role of methane clathrate destabilization in triggering large-scale global warming in the Earth's climatic history, as evidenced by the carbon $\delta^{13}C$ excursion in the geologic record. Notable among these incidents were the warming epochs during the Permian-Triassic boundary (about 252 million years ago) and the Paleocene-Eocene thermal maximum (about 55 million years ago). It has been hypothesized that CO_2-driven ocean circulation changes (Lunt et al., 2010) could have amplified the Paleocene-Eocene thermal maximum clathrate destabilization (Archer, 2007; Archer et al., 2009), although such a release might have occurred chronically over thousands of years rather than as a single catastrophic event. In another study (Lunt et al., 2011) it is postulated that the multiple rapid warmings during the Paleogene

ACPD
12, 26477–26502, 2012

(specifically the Paleocene and Eocene periods spanning 59 to 50 million years ago) resulted from methane clathrate destablizations triggered by nonlinear interactions between the climate and the carbon cycle that modulated the effect of orbital variations.

Worryingly, there have been recent observational studies, mainly confined to the Arctic region, observing fluxes of methane into the ocean and atmosphere that are likely to be from clathrates and/or relic permafrost. Field investigations (Westbrook et al., 2009) have observed substantial methane gas plumes emanating from the seafloor along the Spitsbergen continental slope at depths of 150–400 m, which is where models predict the first evidence of clathrate release will be seen (Reagan and Moridis, 2009), although a study (Fisher et al., 2011) of the isotopic evidence of methane in Arctic air found that such methane plumes have not yet reached the atmosphere. Extensive venting of methane from the East Siberian Arctic Shelf has also been observed (Shakhova et al., 2010), with bubbles reaching the atmosphere through the shallow ocean and producing large increases in atmospheric methane concentration as measured on the ship. In another study (Biastoch et al., 2011), an analysis of Arctic bottom water temperatures under a projected warming scenario suggests that the strongest impact will be on the shallow regions affected by Atlantic inflow where methane clathrates are most sensitive to dissociation, with consequences for ocean acidification and oxygen depletion in the water column (Elliott et al., 2011a).

A recent study (Reagan et al., 2011a,b) estimates the methane released into the water column from methane clathrates over the entire Arctic basin will be in the range 1600 to 8000 Tg(CH_4) in the century following the appearance of methane plumes, with an additional 4300 to 22 000 Tg(CH_4) over the subsequent two centuries even if there is no further increase in ocean bottom temperature. In this paper we present results from a model sensitivity study based on one of these scenarios, and analyze its impact on the global atmosphere using the state-of-the-art CESM model with an interactive atmospheric chemistry component and fully active physical ocean. The paper is organized in five sections. Section 2 gives the details of models, method and data used

ACPD
12, 26477–26502, 2012

for this analysis. Sections 3 and 4 describe and analyze the data obtained from the simulation. Conclusions are presented in Sect. 5.

2 Models, methods, and data

We performed our simulations with the CESM model (Gent et al., 2011), which is a state-of-the-art global climate model that includes interactive atmosphere, land, ocean, sea-ice, biogeochemistry, and atmospheric chemistry components. The code and documentation are available at http://www.cesm.ucar.edu/. The specific version used in this study is a modified version of CESM 1.0 beta 14. The specific configuration used was B2000CNchem, which uses the Community Atmosphere Model version 4 (CAM4) for the atmospheric component, the Community Land Model (CLM) with the Carbon-Nitrogen biogeochemical model for the land component, the Parallel Ocean Program version 2 (POP2) for the ocean component, Community Ice CodE (CICE) for the sea-ice component, and CAM-CHEM with a "fast" chemistry mechanism for the atmospheric chemistry component. The resolution was 1.9×2.5 degrees for the atmosphere and approximately one degree for the ocean. We modified the atmospheric radiation code to include the short-wave absorption effects of methane (Collins et al., 2006).

The chemical reaction set in CAM-chem (Lamarque et al., 2012) was replaced with a simplified version of the chemical reaction set of the IMPACT off-line chemistry model (Rotman et al., 2004), which was designed to simulate both the troposphere and stratosphere and, most critically for this work, to handle methane emissions rather than a concentration boundary condition. The specific reaction set is a "fast" version of the "full" IMPACT reaction set, comprising just 28 species, 52 thermal reactions and 19 photolysis reactions (Cameron-Smith et al., 2006) in which the effects of non-methane hydrocarbons and halogens are ignored in order to reduce the computational cost and make the multi-century simulations presented in this work feasible. The chemical performance of this "fast" mechanism was validated by comparison with the full reaction

ACPD
12, 26477–26502, 2012

set, and included tests of the chemical response to perturbations in the emission of methane (CH_4), carbon mono-oxide (CO), and nitrogen oxides (NO_x).

The TOUGH + HYDRATE code (Moridis et al., 2008) used to generate our ocean methane flux scenarios simulated multiphase flow and transport in clathrate-bearing geologic media. It included coupled mass and energy transport within porous media, and described the full phase behavior of water, methane, solid clathrate, ice, and inhibitor species. The code was used to simulate disperse, low-saturation (stratigraphic) deposits with a uniform initial clathrate saturation of 0.03, reflecting the high end of the estimated global average saturation for such deposits. At each depth and location it simulated a 1-D domain describing the sediment column from the seafloor downward, and was initialized at thermal, chemical, and hydrostatic equilibrium for each depth and temperature. Using plausible physical parameters for the sediments and for the simulations, the 1-D model was integrated over the Arctic basin (Reagan et al., 2011a,b) and the Sea of Okhotsk using a 4-min ETOPO2 bathymetric grid, at 50 m depth intervals from 300 m to 700 m.

The predicted emissions are not a simple function of the warming. Rather, in response to gradual warming at the sea-floor, there is no significant methane release for a few decades while the heat propagates into the sediment and the methane works its way back up to the sea-floor. There is then an abrupt increase in the emission rate, followed by a slow decline, such that it can be crudely approximated by a step function (see Fig. 1). In order to do our sensitivity study we selected an emission rate that was representative of one of the higher emission scenarios: +5 °C per century at 350 m, +3 °C per century at 400–600 m, and +1 °C per century below 600 m. Specifically, for our simulation with enhanced Arctic emissions we added 139 $Tg(CH_4)\,yr^{-1}$ to the regular atmospheric methane sources in our present-day control. Note that this is actually around 10 % more than we intended because CESM uses bi-linear interpolation to convert from the provided emission grid to the atmosphere grid, which is non-conservative, especially with point sources, but this difference is within the emission uncertainties.

ACPD
12, 26477–26502, 2012

Not all of the methane leaving the sediment will make it to the atmosphere. Some previous studies have suggested the fraction of methane from clathrates that reaches the surface is only about 1 % (Lamarque, 2008; Elliott et al., 2011a). However, a more recent modeling study shows that as much as 80–100 % of the dissociated methane might reach the atmosphere (Elliott et al., 2011b) if ocean methanotrophs become nutrient limited, or the methane bubbles rise higher in the ocean from which the methane will vent to the atmosphere more quickly. Because ocean and sediment losses are very uncertain, with estimates ranging from almost no loss to almost total loss, we chose to ignore these losses, i.e. we assumed 100 % transmission of methane from seafloor to atmosphere. We did this because our primary goal was a sensitivity study, and the uncertainty in sea-floor emissions is large enough that any error in our assumed transmission may be compensated for by a larger than expected sea-floor emission. Part of the emission uncertainty comes from the fact that there are also other sources of methane in the northern high latitudes that are sensitive to warming, such as the northern lakes, wetlands, rivers, East Siberian continental shelf, and thawing permafrost regions, which would have a very similar effect on our model to our clathrate emissions.

To study the climate impact of our methane release from Arctic clathrates, we ran two long climate simulations (about 539 yr for the control and 499 yr for the Arctic emission case) using the fully coupled ocean-atmosphere-land CESM model with interactive atmospheric chemistry described above. The control simulation (C) used an estimate of the present-day distribution and magnitude of methane emissions. The Arctic emission simulation (AE) differed only in the addition of 139 $Tg(CH_4)\,yr^{-1}$ in atmospheric methane emissions over the Arctic and Sea of Okhotsk. Comparing the output of these two simulations provided an estimate of the impact of our clathrate emission scenario that is analyzed in the sections below.

Methane is a long-lived gas, whose molecules reside in the atmosphere for about 9 yr on average before they are destroyed (IPCC AR4: Solomon et al., 2007). Because the total emission and destruction rates for methane in the present-day are only known to an accuracy of about 15 % (IPCC AR4: Solomon et al., 2007) but the resultant

ACPD
12, 26477–26502, 2012

concentration for present-day atmosphere is known very accurately, we first scaled the emissions for the control simulation to ensure that the methane concentration simulated by the model was close to the currently observed value. Specifically, we achieved an average surface mixing ratio of 1.79×10^{-6} mol mol^{-1} of CH_4 at steady-state in our control run, which is comparable to recent observations (Rigby et al., 2008; Dlugokencky et al., 2009), with 629 Tg(CH_4) yr^{-1}, which is at the upper end of recent estimates (IPCC AR4: Solomon et al., 2007). After the control run reached steady state in atmospheric CH_4 concentration and temperature (about 70 yr), the simulations for the Arctic Emission case (hereafter referred to as AE) branched from the control run (hereafter referred to as C). We discarded a further 50 yr of spin-up in both simulations so the AE simulation could reach a new equilibrium, and we saw no impact of any deep ocean drift. This left 449 and 420 yr in steady state to analyze for the AE and C cases, respectively. The extra methane from the Arctic sediment model of 139 Tg(CH_4) yr^{-1} (a 22 % increase in the global total) was added to the control emission in 3 specific locations that corresponded to the three largest predicted emission locations, which were in the Barents Sea, Canadian Archipelago, and Sea of Okhotsk in approximately the ratio 5 : 5 : 1 (the precise locations are shown in Fig. 2).

We do not claim that this is the most likely scenario because there is still a lot of uncertainty in the magnitude and location of possible methane releases from clathrates, including the extent to which methane may be destroyed in the ocean before it reaches the atmosphere. However we do consider this to be a plausible scenario. This scenario is also comparable to plausible scenarios for other methane reservoirs (e.g. decaying permafrost, wetlands, rice, fracking), so many of our results should have a broad application.

3 Response of annual mean quantities to clathrate emissions

Our simulation results show the potential impact the extra methane emissions could have, from the scenario described in the previous section, on surface methane,

ACPD
12, 26477–26502, 2012

temperature, ozone and precipitation, which we will present by examining the mean, percentage difference, standard deviation, and signal-to-noise (SNR) ratio at the Earth's surface for the annual means of each variable. Annual means have the advantage that they are less noisy than seasonal means, and the timing of seasonal impacts depends on location. However, any seasonal effects will be muted in the annual-mean, so seasonal impacts will be larger than indicated by our figures.

The increase in surface methane concentration between the Arctic emission case (AE) and the control case (C) is shown in Fig. 2a. As expected, we see increases everywhere. Because of the high values near the clathrate emission locations, and the smoothness of the field over most of the rest of the planet, it is hard to find a color scale that clearly conveys the distribution. A clearer understanding may be gained from Fig. 2e, which shows the zonal mean of the data. It can be seen that there is a significant enhancement in the Northern Hemisphere, in spite of the long-lifetime of methane. Figure 2b, c shows the percentage increase in surface methane concentration for the AE case with respect to the control, with Fig. 2c using a finer scale to show more features. These results show about a 38 % increase in the global mean surface concentration of methane although clearly there are regions with even higher percentage increases in the Northern Hemisphere, and the Arctic in particular. This is almost double the percentage increase in the methane emissions, which was about 22 %. A nonlinear response is expected due to the fact that as methane reacts with the hydroxyl radical (OH) in the atmosphere the concentration of OH in the atmosphere decreases, reducing the main chemical loss of methane and thereby increasing the lifetime of CH_4 (Prather, 1996). However, our simulation is fully interactive, so our change includes temperature and water-vapor feedbacks as well. The temporal standard deviation of the annual-mean methane concentration in the AE scenario is shown in Fig. 2d, where the scale has been chosen to reveal features in regions other than the Arctic. This increase in interannual variability has broadly the same pattern as the mean increase, but as will be shown more clearly in section 4, the increase in variability is greater than would be expected due to the increase in the mean alone. Note that the standard

ACPD
12, 26477–26502, 2012

deviation of the annual-mean methane concentration is entirely equivalent to the standard deviation of the difference between the AE and C simulations if the long-term mean of the control is used, since there will be no contribution to the variability from the C simulation.

The difference in annually averaged surface temperature between AE and C in Fig. 3a shows a definite pattern of greater warming at high latitudes and, to a lesser extent, over land, with a global mean temperature increase of about 0.2 K, and regions near the poles where the temperature increases by over 0.5 K. This is the same general pattern that is seen in response to radiative forcing from a uniform CO_2 increase. The additional simulations necessary to determine whether our clathrate methane response is different from the standard CO_2 response are currently underway, but are not far enough advanced at the time of writing to determine, for example, whether the Arctic warming is further enhanced by the excess methane in the region. Figure 3b shows the mean percentage increase in surface temperature of AE relative to C. The pattern is broadly similar to the pattern of the raw difference, but is slightly increased at the poles because of the colder temperatures in the control base state. Figure 3c shows the temporal standard deviation of the annually averaged temperature difference of the AE simulation. Just like the control simulation (not shown), the variability in the temperature difference is greater in the polar regions compared to lower-latitudes. This raises the question of whether the larger mean temperature differences at the poles could be the result of chance. A basic test is to perform a point-wise z-test using the signal to noise ratio (SNR) of the temperature increase, which is computed by dividing the mean temperature difference in each gridcell by the standard error of the timeseries in the same gridcell (i.e. the temporal standard deviation divided by square root of the number of time points, assuming independence). This SNR is shown in Fig. 3d and shows that the SNR at the poles is indeed generally less than at lower latitudes, even though the signal is greater at the poles, because of the smaller interannual variability at lower latitudes, but the SNR is still generally greater than 3 over the poles, indicating the change is statistically significant almost everywhere.

ACPD
12, 26477–26502, 2012

Next we show the changes in surface ozone concentration due to our Arctic clathrate emissions. Figure 4a shows the difference in annually averaged ozone between AE and C. An increase in ozone is observed everywhere, but is particularly enhanced in urban areas with already poor air quality. Urban areas generate more nitrogen oxides, in the presence of which tropospheric methane oxidizes and produces ozone (Fiore et al., 2008). Interestingly, we also see an increase in ozone concentration over the Himalayan Plateau. The reason for this is unclear. We see no evidence that this is a chemical response, so it is presumably the response of some dynamical change, such as increased downwelling of ozone from the stratosphere, but we do not have the diagnostics to confirm this in our current simulations. The percentage increase in surface ozone concentration for the AE case with respect to the control is shown in Fig. 4b. Although the percentage difference in surface ozone concentration shows higher values in more polluted regions as expected, there are also differences of 10 % or more in regions over the equatorial oceans that are larger than the increases over the extratropical ocean regions. It is not clear whether the differences between the tropical and extratropical oceans are a dynamical, chemical or combined effect. Overall then, our Arctic clathrate emission increases the global methane emission by about 22 %, which produces a global increase of 39 % in surface CH_4 concentration, which in turn increases the mean surface ozone concentration by 10 % (and more in urban areas). This highlights one way that global air quality is inter-related with global climate change (Fiore et al., 2012). Figure 4c shows the temporal standard deviation of the difference in ozone concentration that leads to the signal to noise ratio for the increase in surface ozone concentration in Fig. 4d, which shows that the mean changes discussed above are clearly statistically significant, with SNRs of over 100 over polluted regions and SNRs around 20 over equatorial regions.

The changes in precipitation between the AE and C cases are shown in Fig. 5. But note that the color scheme has been chosen to indicate the increased precipitation in blue and decreased precipitation in brown, which is the opposite color convention to our other figures. We did this because blue and brown are commonly associated with

ACPD
12, 26477–26502, 2012

abundant water and drought, respectively. The raw and percentage increases in mean precipitation in the AE case relative to the C case are shown in Fig. 5a, b. They show a pattern of increased and decreased precipitation, but it isn't immediately clear what is significant. Figure 5c shows the standard deviation of the difference in precipitation, which highlights the large internal interannual variability in precipitation compared to the changes seen in the mean. However, in the SNR plot, Fig. 5d, the pattern seen in the CMIP3 intercomparison (IPCC AR4: Solomon et al., 2007) can be seen, namely increased precipitation at high latitudes and a more complex pattern at lower latitudes. But a word of caution must be added here because the absolute value of our SNR is rarely greater than 3.

4 Response of variability to clathrate emissions

In addition to the mean changes caused by the methane clathrate emissions in our model, we also see changes in the interannual variability of some of the quantities, particularly the methane and ozone concentrations. The ratio of the standard deviation in the AE case to the corresponding standard deviation in the control case for methane, temperature, ozone, and precipitation is shown in Fig. 6. The ratio of the standard deviations for methane is shown in Fig. 6a. The northern high latitudes show very high variability ratios, with the variability in the AE case being tens of times greater than in the C case, especially near where the clathrate emissions were introduced. This increase in variability must be because of dynamical variability blowing the downwind plume around, because the chemical lifetime of methane is too long for it to be primarily a chemical effect. In order to see the changes in variability over the rest of the planet, the same quantity is reproduced with a finer scale in Fig. 6b. This plot shows ratios over 1.5 for most regions, i.e. over 50 % increases. When compared to Fig. 2c, it is clear that the variability has increased by more than it would have if the response to the clathrate emissions was a simple scaling of the concentration field, i.e. the mean and variation of methane concentration are affected differently by the clathrate emissions.

ACPD
12, 26477–26502, 2012

Of course, it is necessary to know whether any change in the variability is statistically significant. We can estimate the uncertainty in each standard deviation ratio using standard statistical error analysis as follows. The estimated uncertainty in a standard deviation s is given by $\frac{1}{\sqrt{2(n-1)}} < s^2 >$ for a sufficiently long time series that has a Gaussian distribution, where $< s^2 >$ denotes the expectation of the variance, and n is the number of independent time points (Squires, 1991). For a sufficiently long time series, the $(n-1)$ term in the above expression can be well approximated by n. If R denotes the ratio of two standard deviations, then $(\frac{\Delta R}{R})$ denotes the relative uncertainty in it, and can be derived from the uncertainty in the individual standard deviations using the usual rules for calculating the uncertainty in a ratio:

$$\frac{\Delta R}{R} = \sqrt{\left(\frac{\Delta\sigma_{\mathrm{AE}}}{\sigma_{\mathrm{AE}}}\right)^2 + \left(\frac{\Delta\sigma_{\mathrm{C}}}{\sigma_{\mathrm{C}}}\right)^2} = \sqrt{\left(\frac{\frac{\sigma_{AE}}{\sqrt{2n}}}{\sigma_{\mathrm{AE}}}\right)^2 + \left(\frac{\frac{\sigma_{\mathrm{C}}}{\sqrt{2n}}}{\sigma_{\mathrm{C}}}\right)^2} = \sqrt{(\frac{1}{2n} + \frac{1}{2n})} = \frac{1}{\sqrt{n}}, \qquad (1)$$

Thus, we see that the uncertainty in the ratio is dependent only on the number of years in our time series. Hence, with time-series of over 400 yr the 1-sigma uncertainty in the ratio of the standard deviations of AE to C turns out to be about 5 %. Returning to the increase in methane variability, we now see that in most locations the increase in variability is over 3-sigma greater than the increase in the mean alone would imply.

In Fig. 6c we see the ratio of the standard deviations for surface temperature of AE compared to C. We see increases and decreases of up to 10 %, or so, in variability, so most locations are not significant at the 2-sigma level. There are regions with larger changes in variability, but with so many locations it is always expected that there will be a few places that exceed a 2-sigma change, so it is hard to say whether there is any significant change in variability for temperature.

Figure 6d shows the ratio of standard deviations for the surface concentration of ozone. Perhaps surprisingly, the increase in variability in surface ozone is not necessarily greatest in polluted regions. The variability seems to increase most in the Southern

ACPD
12, 26477–26502, 2012

Hemisphere oceans, although there is an increase over most of the planet. After consideration of the increase in the mean, Fig. 4b, and the uncertainty in the ratio, there are many regions that are not significant at the 2-sigma level, but there are still many regions that are significant. It is also noteworthy that nearly all locations show greater variability than the increase in the mean would suggest, even if they are not individually statistically significant. Hence, it would appear that the ozone variability does increase, which is not surprising given that the methane variability increased and ozone creation is sensitive to methane concentrations.

Figure 6e shows the ratio of standard deviations for precipitation. As with temperature, we see that the changes in variability include both increases and decreases that are mostly within the 2-sigma range. The only region that might be showing a significant change is the decrease in precipitation variability in the model's El Nino dry tongue region in the eastern tropical Pacific, which is about 2-sigma greater than the mean drying.

5 Conclusion and discussion

The previous sections presented the predicted consequences of a "what if" scenario for release of methane from Arctic clathrates that is plausible, considering the uncertainties in the estimates of clathrate abundance, release rate, and consumption in the ocean. However, there are other potential sources of additional methane comparable to our scenario, including natural gas production by hydraulic fracturing (fracking), rice production, ruminant farming, and other natural Arctic sources such as wetlands, methane trapped below relic permafrost (e.g. the East Siberian Arctic Shelf), and thermokarst lakes. Recent research (Wadham et al., 2012) also suggests there is a large amount of methane clathrates beneath the Antarctic ice shelves that could be vulnerable to warming. Hence, it is likely that a scenario similar to the one we simulated will occur from some combination of these sources, and it is possible within the uncertainties of all these sources for methane emissions to get much larger, with

ACPD
12, 26477–26502, 2012

consequently greater impacts, unless methane is closely monitored and mitigation actions taken if necessary.

Of the changes between our simulations with and without Arctic clathrate emissions, the non-linear increase in methane concentration, and the spatial patterns of temperature, ozone, and precipitation increases, were broadly in line with our prior expectations. However, the size of the spatial inhomogeneity induced in the methane concentration by the Arctic emissions, and the increases in variability of methane and ozone throughout the globe, have not been previously reported, to our knowledge. The importance of these changes may be magnified because of the non-linear processes they interact with, such as sea-ice melting and exceedance of ozone air-quality standards. The ability to study such changes in variability is one of the important reasons for performing simulations with atmospheric chemistry integrated into a climate model with a full ocean model.

In order to study the potential reinforcement between the methane sources susceptible to changes in temperature and precipitation (i.e. wetlands, permafrost, and clathrates), in which warming and precipitation changes caused by one methane source will feed back onto the emissions from it and the other sources, it will be necessary to couple our model to interactive models for wetlands, permafrost, clathrates, bubble rise, and the ocean methane cycle. This will let us estimate the feedback amplification factors between the different methane sources. For reference, a model study (Bohn et al., 2007) found that an increase of temperature by 3 °C in conjunction with a 10 % increase in precipitation in the Western Siberian region of wetlands could lead to doubling of annual methane emissions.

Additional simulations with a globally uniform CO_2 concentration equivalent to our methane clathrate forcing will allow us to determine whether, or not, the Arctic enhancements we see in temperature and precipitation with our Arctic clathrate methane emissions are quantitatively enhanced above the usual response simulated for uniform greenhouse gas forcing by the non-uniform methane concentration. The response of

ACPD
12, 26477–26502, 2012

sea-ice and the stratosphere also remain to be examined, so there is still much to be understood about the impact of Arctic methane emissions on the Earth system.

Acknowledgement. This work was sponsored by the US Department of Energy (BER), performed under the auspices of the US Department of Energy by Lawrence Livermore National Laboratory under Contract DE-AC52-07NA27344, and used resources of the National Energy Research Scientific Computing Center, which is supported by the Office of Science of the US Department of Energy under Contract No. DE-AC02-05CH11231.

References

Archer, D.: Methane hydrate stability and anthropogenic climate change, Biogeosciences, 4, 521–544, doi:10.5194/bg-4-521-2007, 2007.

Archer, D., Buffett, B., and Brovkin, V.: Ocean methane hydrates as a slow tipping point in the global carbon cycle, P. Natl. Acad. Sci. USA, 106, 20596–20601, doi:10.1073/pnas.0800885105, 2009.

Biastoch, A., Treude, T., Ruepke, L. H., Riebesell, U., Roth, C., Burwicz, E. B., Park, W., Latif, M., Boening, C. W., Madec, G., and Wallmann, K.: Rising Arctic Ocean temperatures cause gas hydrate destabilization and ocean acidification, Geophys. Res. Lett., 38, L08602, doi:10.1029/2011gl047222, 2011.

Bohn, T. J., Lettenmaier, D. P., Sathulur, K., Bowling, L. C., Podest, E., McDonald, K. C., and Friborg, T.: Methane emissions from western Siberian wetlands: heterogeneity and sensitivity to climate change, Environ. Res. Lett., 2, 045015, doi:10.1088/1748-9326/2/4/045015, 2007.

Buffett, B. and Archer, D.: Global inventory of methane clathrate: sensitivity to changes in the deep ocean, Earth Planet. Sci. Lett., 227, 185–199, doi:10.1016/j.epsl.2004.09.005, 2004.

Cameron-Smith, P., Lamarque, J. F., Connell, P., Chuang, C., and Vitt, F.: Toward an Earth system model: atmospheric chemistry, coupling, and petascale computing, in: Scidac 2006: Scientific Discovery through Advanced Computing, 2006.

Collins, W. D., Ramaswamy, V., Schwarzkopf, M. D., Sun, Y., Portmann, R. W., Fu, Q., Casanova, S. E. B., Dufresne, J. L., Fillmore, D. W., Forster, P. M. D., Galin, V. Y., Gohar, L. K., Ingram, W. J., Kratz, D. P., Lefebvre, M. P., Li, J., Marquet, P., Oinas, V., Tsushima, Y., Uchiyama, T., and Zhong, W. Y.: Radiative forcing by well-mixed greenhouse gases: estimates from climate models in the Intergovernmental Panel on Climate

ACPD

12, 26477–26502, 2012

Change (IPCC) Fourth Assessment Report (AR4), J. Geophys. Res.-Atmos., 111, D14317, doi:10.1029/2005jd006713, 2006.
Dlugokencky, E. J., Bruhwiler, L., White, J. W. C., Emmons, L. K., Novelli, P. C., Montzka, S. A., Masarie, K. A., Lang, P. M., Crotwell, A. M., Miller, J. B., and Gatti, L. V.: Observational constraints on recent increases in the atmospheric CH(4) burden, Geophys. Res. Lett., 36, L18803, doi:10.1029/2009gl039780, 2009.
Elliott, S., Reagan, M., Moridis, G., and Cameron-Smith, P.: Geochemistry of clathrate-derived methane in Arctic ocean waters, Geophys. Res. Lett., 37, 12607–12607, 2010.
Elliott, S., Maltrud, M., Reagan, M., Moridis, G., and Cameron-Smith, P.: Marine methane cycle simulations for the period of early global warming, J. Geophys. Res.-Biogeosci., 116, G01010, doi:10.1029/2010jg001300, 2011a.
Elliott, S., Maltrud, M., Reagan, M., Moridis, G., and Cameron-Smith, P.: Correction to "Marine methane cycle simulations for the period of early global warming", J. Geophys. Res., 116, G03007, doi:10.1029/2011JG001725, 2011b.
Fiore, A. M., West, J. J., Horowitz, L. W., Naik, V., and Schwarzkopf, M. D.: Characterizing the tropospheric ozone response to methane emission controls and the benefits to climate and air quality, J. Geophys. Res., 113, D08307, doi:10.1029/2007JD009162, 2008.
Fiore, A. M., Naik, V., Spracklen, D. V., Steiner, A., Unger, N., Prather, M., Bergmann, D., Cameron-Smith, P. J., Cionni, I., Collins, W. J., Dalsoren, S., Eyring, V., Folberth, G. A., Ginoux, P., Horowitz, L. W., Josse, B., Lamarque, J.-F., MacKenzie, I. A., Nagashima, T., O'Connor, F. M., Righi, M., Rumbold, S. T., Shindell, D. T., Skeie, R. B., Sudo, K., Szopa, S., Takemura, T., and Zeng, G.: Global air quality and climate, Chem. Soc. Rev., 41, 6663–6683, doi:10.1039/C2CS35095E, 2012.
Fisher, R. E., Sriskantharajah, S., Lowry, D., Lanoisellé, M., Fowler, C. M. R., James, R. H., Hermansen, O., Lund Myhre, C., Stohl, A., Greinert, J., Nisbet-Jones, P. B. R., Mienert, J., and Nisbet, E. G.: Arctic methane sources: isotopic evidence for atmospheric inputs, Geophys. Res. Lett., 38, L21803, doi:10.1029/2011gl049319, 2011.
Gent, P. R., Danabasoglu, G., Donner, L. J., Holland, M. M., Hunke, E. C., Jayne, S. R., Lawrence, D. M., Neale, R. B., Rasch, P. J., Vertenstein, M., Worley, P. H., Yang, Z. L., and Zhang, M. H.: The community climate system model version 4, J. Climate, 24, 4973–4991, doi:10.1175/2011jcli4083.1, 2011.
Gornitz, V. and Fung, I.: Potential distribution of methane hydrates in the worlds oceans, Global Biogeochem. Cy., 8, 335–347, doi:10.1029/94gb00766, 1994.

ACPD
12, 26477–26502, 2012

Isaksen, I. S. A., Gauss, M., Myhre, G., Anthony, K. M. W., and Ruppel, C.: Strong atmospheric chemistry feedback to climate warming from Arctic methane emissions, Global Biogeochem. Cy., 25, Gb2002, doi:10.1029/2010gb003845, 2011.

Kennett, J. P., Cannariato, K. G., Hendy, I. L., and Behl, R. J.: Carbon isotopic evidence for methane hydrate instability during quaternary interstadials, Science, 288, 128–133, 2000.

Klauda, J. B. and Sandler, S. I.: Global distribution of methane hydrate in ocean sediment, Energy & Fuels, 19, 459–470, 10.1021/ef049798o, 2005.

Lamarque, J.-F.: Estimating the potential for methane clathrate instability in the 1 %-CO(2) IPCC AR-4 simulations, Geophys. Res. Lett., 35, L19806, doi:10.1029/2008gl035291, 2008.

Lamarque, J. F., Kiehl, J. T., Shields, C. A., Boville, B. A., and Kinnison, D. E.: Modeling the response to changes in tropospheric methane concentration: application to the Permian-Triassic boundary, Paleoceanography, 21, PA3006, doi:10.1029/2006pa001276, 2006.

Lamarque, J. F., Kiehl, J. T., and Orlando, J. J.: Role of hydrogen sulfide in a Permian-Triassic boundary ozone collapse, Geophys. Res. Lett., 34, L02801, doi:10.1029/2006GL028384, 2007.

Lamarque, J.-F., Emmons, L. K., Hess, P. G., Kinnison, D. E., Tilmes, S., Vitt, F., Heald, C. L., Holland, E. A., Lauritzen, P. H., Neu, J., Orlando, J. J., Rasch, P. J., and Tyndall, G. K.: CAM-chem: description and evaluation of interactive atmospheric chemistry in the Community Earth System Model, Geosci. Model Dev., 5, 369–411, doi:10.5194/gmd-5-369-2012, 2012.

Lunt, D. J., Valdes, P. J., Dunkley Jones, T., Ridgwell, A., Haywood, A. M., Schmidt, D. N., Marsh, R., and Maslin, M.: CO_2-driven ocean circulation changes as an amplifier of Paleocene-Eocene thermal maximum hydrate destabilization, Geology, 38, 875–878, doi:10.1130/g31184.1, 2010.

Lunt, D. J., Ridgwell, A., Sluijs, A., Zachos, J., Hunter, S., and Haywood, A.: A model for orbital pacing of methane hydrate destabilization during the Palaeogene, Nature Geosci, 4, 775–778, available at: http://www.nature.com/ngeo/journal/v4/n11/abs/ngeo1266.html#supplementary-information (last access: October 2012), 2011.

Maslin, M., Owen, M., Betts, R., Day, S., Dunkley Jones, T., and Ridgwell, A.: Gas hydrates: past and future geohazard?, Philos. T. Roy. Soc. A, 368, 2369–2393, doi:10.1098/rsta.2010.0065, 2010.

Milkov, A. V.: Global estimates of hydrate-bound gas in marine sediments: how much is really out there?, Earth-Sci. Rev., 66, 183–197, doi:10.1016/j.earscirev.2003.11.002, 2004.

ACPD
12, 26477–26502, 2012

Moridis, G. J., Kowalsky, M. B., and Pruess, K.: TOUGH+HYDRATE v1.0 User's Manual: A Code for the Simulation of System Behavior in Hydrate-Bearing Geologic Media, available at: http://esd.lbl.gov/files/research/projects/tough/documentation/TplusH_Manual_v1.pdf (last access: October 2012), Report LBNL-0149E, Lawrence Berkeley National Laboratory, Berkeley, CA, 2008.

Prather, M. J.: Time scales in atmospheric chemistry: theory, GWPs for CH_4 and CO, and runaway growth, Geophys. Res. Lett., 23, 2597–2600, doi:10.1029/96gl02371, 1996.

Reagan, M., and Moridis, G. J.: Oceanic gas hydrate instability and dissociation under climate change scenarios, Geophys. Res. Lett., 34, L22709, doi:10.1029/2007gl031671, 2007.

Reagan, M. and Moridis, G. J.: Dynamic response of oceanic hydrate deposits to ocean temperature change, J. Geophys. Res.-Oceans, 113, C12023, doi:10.1029/2008jc004938, 2008.

Reagan, M. and Moridis, G. J.: Large-scale simulation of methane hydrate dissociation along the West Spitsbergen Margin, Geophys. Res. Lett., 36, L23612, doi:10.1029/2009gl041332, 2009.

Reagan, M., Moridis, G., Elliott, S. M., Maltrud, M., and Cameron-Smith, P.: Basin-scale assesment of gas hydrate dissociation in response to climate change, Edinburgh, Scotland, UK, 2011a.

Reagan, M. T., Moridis, G. J., Elliott, S. M., and Maltrud, M.: Contribution of oceanic gas hydrate dissociation to the formation of Arctic Ocean methane plumes, J. Geophys. Res., 116, C09014, doi:10.1029/2011JC007189, 2011b.

Rigby, M., Prinn, R. G., Fraser, P. J., Simmonds, P. G., Langenfelds, R. L., Huang, J., Cunnold, D. M., Steele, L. P., Krummel, P. B., Weiss, R. F., O'Doherty, S., Salameh, P. K., Wang, H. J., Harth, C. M., Mühle, J., and Porter, L. W.: Renewed growth of atmospheric methane, Geophys. Res. Lett., 35, L22805, doi:10.1029/2008gl036037, 2008.

Rotman, D. A., Atherton, C. S., Bergmann, D. J., Cameron-Smith, P. J., Chuang, C. C., Connell, P. S., Dignon, J. E., Franz, A., Grant, K. E., Kinnison, D. E., Molenkamp, C. R., Proctor, D. D., and Tannahill, J. R.: IMPACT, the LLNL 3-D global atmospheric chemical transport model for the combined troposphere and stratosphere: model description and analysis of ozone and other trace gases, J. Geophys. Res., 109, D04303, doi:10.1029/2002jd003155, 2004.

Shakhova, N., Semiletov, I., Salyuk, A., Yusupov, V., Kosmach, D., and Gustafsson, O.: Extensive methane venting to the atmosphere from sediments of the East Siberian Arctic Shelf, Science, 327, 1246–1250, doi:10.1126/science.1182221, 2010.

ACPD
12, 26477–26502, 2012

Solomon, S., Qin, D., Manning, M., Chen, Z., Marquis, M., Averyt, K. B., Tignor, M., and Miller, H. L.: Contribution of Working Group I to the Fourth Assessment Report of the Intergovernmental Panel on Climate Change, 2007, Cambridge University Press, Cambridge, UK and New York, NY, USA, 2007.

Squires, G. L.: Practical Physics, 3rd edn., Cambridge University Press, Cambridge, 1991.

Stolaroff, J. K., Bhattacharyya, S., Smith, C. A., Bourcier, W. L., Cameron-Smith, P. J., and Aines, R. D.: A review of methane mitigation technologies with application to rapid release of methane from the Arctic, Environ. Sci. Technol., doi:10.1021/es204686w, 2012.

Wadham, J. L., Arndt, S., Tulaczyk, S., Stibal, M., Tranter, M., Telling, J., Lis, G. P., Lawson, E., Ridgwell, A., Dubnick, A., Sharp, M. J., Anesio, A. M., and Butler, C. E. H.: Potential methane reservoirs beneath Antarctica, Nature, 488, 633–637, available at: http://www.nature.com/nature/journal/v488/n7413/abs/nature11374.html#supplementary-information (last access: October 2012), 2012.

Westbrook, G. K., Thatcher, K. E., Rohling, E. J., Piotrowski, A. M., Paelike, H., Osborne, A. H., Nisbet, E. G., Minshull, T. A., Lanoiselle, M., James, R. H., Huehnerbach, V., Green, D., Fisher, R. E., Crocker, A. J., Chabert, A., Bolton, C., Beszczynska-Moeller, A., Berndt, C., and Aquilina, A.: Escape of methane gas from the seabed along the West Spitsbergen continental margin, Geophys. Res. Lett., 36, L15608, doi:10.1029/2009gl039191, 2009.

ACPD
12, 26477–26502, 2012

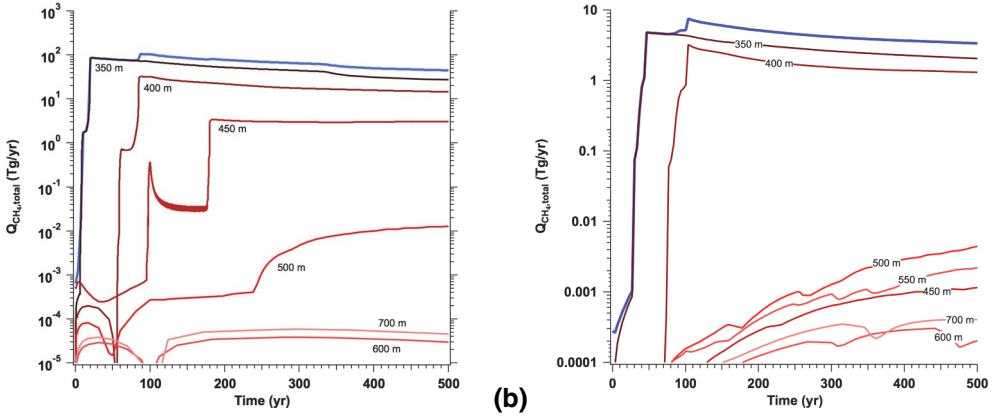

Fig. 1. Simulated flux of CH_4 outgassing from clathrates as a function of depth and time integrated over **(a)** the Arctic Ocean and **(b)** the Sea of Okhotsk. Note that the red lines show the flux for particular depth ranges, and the blue lines show the sum of all the red lines. The emissions have units of $Tg(CH_4)\,yr^{-1}$. This particular scenario assumed ocean bottom temperatures that followed a linear increase of +5 °C per century at 350 m, +3 °C per century at 400–600 m, and +1 °C per century below 600 m, with no further change after the first century.

ACPD
12, 26477–26502, 2012

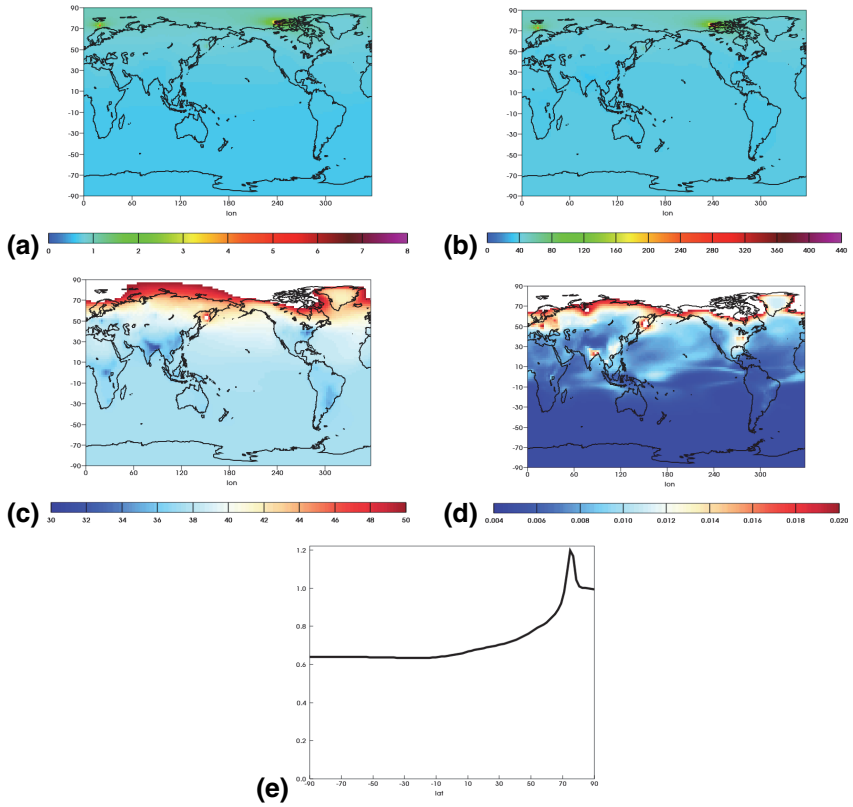

Fig. 2. The change in methane concentration at the surface between the Arctic emission and the control simulations: **(a)** the mean increase (ppmv) of the AE case over the C case, **(b)** the percentage increase of the AE case over the C case, **(c)** the same percentage increase but with a finer scale, **(d)** the standard deviation of the AE case (ppmv), and **(e)** the zonal mean increase in surface concentration of CH_4 from C to AE (ppmv). The arrows in panel **(a)** show the location of the clathrate emissions in our model.

ACPD
12, 26477–26502, 2012

Tropospheric impact of methane emissions from clathrates

S. Bhattacharyya et al.

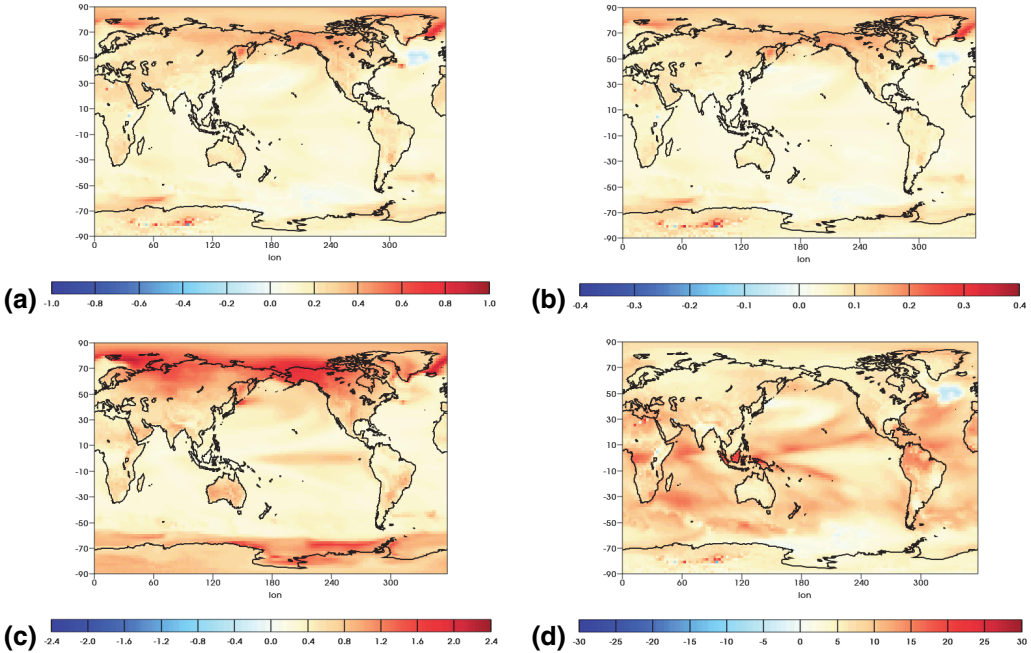

Fig. 3. The change in skin temperature at the surface between the Arctic emission and the control simulations: **(a)** the mean increase (K) of the AE case over the C case, **(b)** the percentage increase of the AE case over the C case, **(c)** the standard deviation of the AE case (K), and **(d)** the signal to noise ratio of the mean increase.

ACPD
12, 26477–26502, 2012

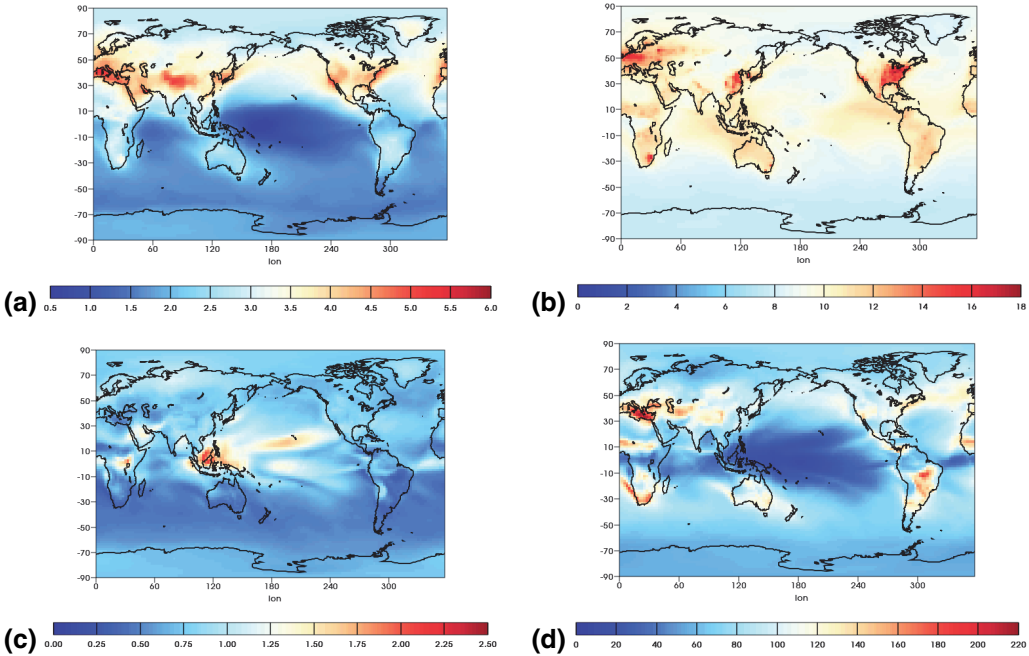

Fig. 4. The change in ozone concentration at the surface between the Arctic emission and the control simulations: **(a)** the mean increase (ppbv) of the AE case over the C case, **(b)** the percentage increase of the AE case over the C case, **(c)** the standard deviation of the AE case (ppbv), and **(d)** the signal to noise ratio of the mean increase.

ACPD
12, 26477–26502, 2012

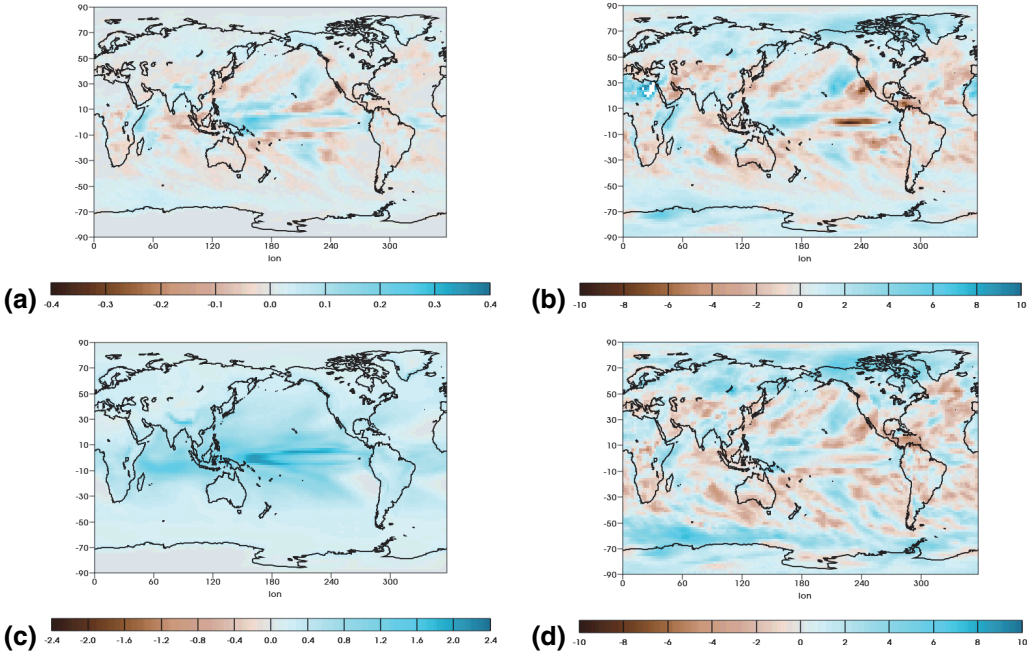

Fig. 5. The change in precipitation at the surface between the Arctic emission and the control simulations: **(a)** the mean increase (mm day^{-1}) of the AE case over the C case, **(b)** the percentage increase of the AE case over the C case, **(c)** the standard deviation of the AE case (mm day^{-1}), and **(d)** the signal to noise ratio of the mean increase.

ACPD
12, 26477–26502, 2012

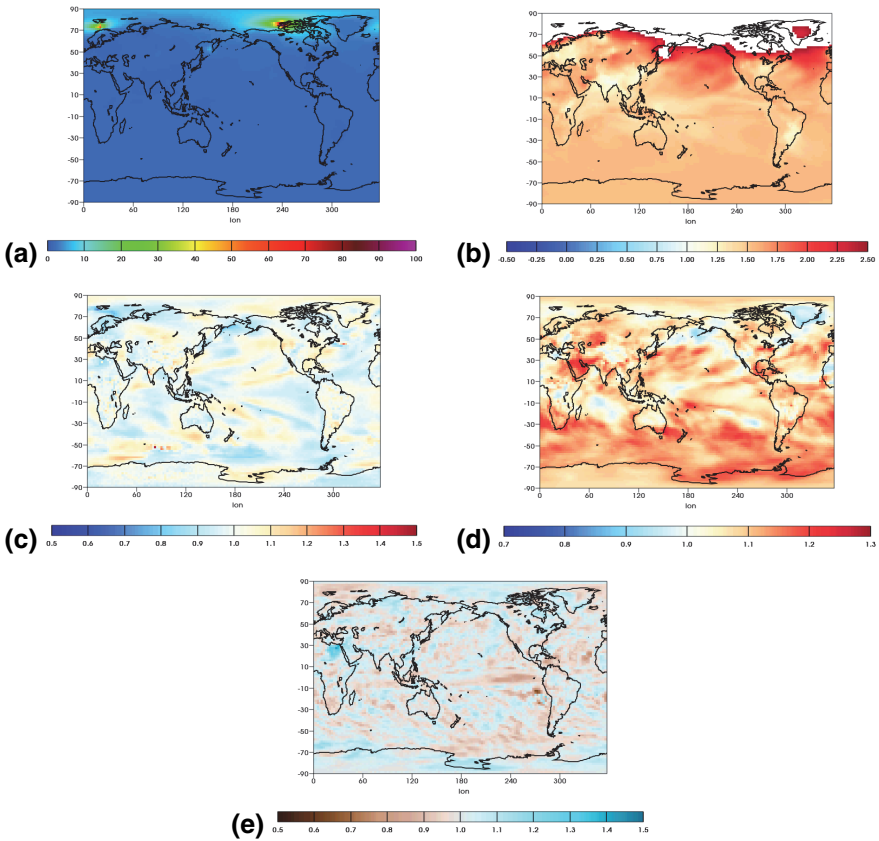

Fig. 6. The ratio of the standard deviations of the Arctic emission case over the control case for **(a)** the surface methane concentration, **(b)** the surface methane concentration at a finer scale, **(c)** the surface skin temperature, **(d)** the surface ozone concentration, and **(e)** the surface precipitation.

ACPD
12, 26477–26502, 2012